Evidence in Support of Lysine 77 and Histidine 96 as Acid−Base Catalytic Residues in Saccharopine Dehydrogenase from Saccharomyces cerevisiae

ARTICLE *in* BIOCHEMISTRY · JANUARY 2012

Impact Factor: 3.02 · DOI: 10.1021/bi201808u · Source: PubMed

6 AUTHORS, INCLUDING:

Vidya Kumar
Henry M Jackson Foundation
17 PUBLICATIONS **137** CITATIONS
SEE PROFILE

Leonard M Thomas
University of Oklahoma
51 PUBLICATIONS **1,271** CITATIONS
SEE PROFILE

Babak Andi
Brookhaven National Laboratory
19 PUBLICATIONS **214** CITATIONS
SEE PROFILE

Ann H West
University of Oklahoma
67 PUBLICATIONS **2,378** CITATIONS
SEE PROFILE

Published in final edited form as:
Biochemistry. 2012 January 31; 51(4): 857–866. doi:10.1021/bi201808u.

Evidence in Support of Lysine 77 and Histidine 96 as Acid-base Catalytic Residues in Saccharopine Dehydrogenase from *Saccharomyces cerevisiae*

Vidya Prasanna Kumar, **Leonard M. Thomas**, **Kostyantyn D. Bobyk**, **Babak Andi**, **Paul F. Cook***, and **Ann H. West***
Department of Chemistry and Biochemistry, University of Oklahoma, 101 Stephenson Parkway, Norman, Oklahoma, 73019

Abstract

Saccharopine dehydrogenase (SDH) catalyzes the final reaction in the α–aminoadipate pathway, the conversion of L-saccharopine to L-lysine (Lys) and α-ketoglutarate (α-Kg) using NAD^+ as an oxidant. The enzyme utilizes a general acid-base mechanism to carry out its reaction with a base proposed to accept a proton from the secondary amine of saccharopine in the oxidation step and group proposed to activate water to hydrolyze the resulting imine. Crystal structures of an open apo-form and a closed form of the enzyme with saccharopine and NADH bound have been solved at 2.0 Å and 2.2 Å resolution, respectively. In the ternary complex, a significant movement of domain I relative to domain II is observed that closes the active site cleft between the two domains and brings H96 and K77 in close proximity to the substrate binding site. The hydride transfer distance is 3.6 Å, and the side chains of H96 and K77 are properly positioned to act as acid-base catalysts. Preparation of the K77 to M, H96 to Q single and the K77M/H96Q double mutant enzymes provide data consistent with their role as the general acid-base catalysts in the SDH reaction. The side chain of K77 initially accepts a proton from the ε-amine of the substrate Lys and eventually donates it to the imino nitrogen as it is reduced to a secondary amine in the hydride transfer step, and H96 protonates the carbonyl oxygen as the carbinolamine is formed. The K77M, H976Q, and K77M/H96Q mutant enzymes give 145-, 28-, and 700-fold decreases in V/E_t and $>10^3$ increases in $V_2/K_{Lys}\mathbf{E_t}$ and $V_2/K_{\alpha\text{-}Kg}\mathbf{E_t}$ (the double mutation gives $>10^5$-fold decreases in the second order rate constants). In addition, the K77M mutant enzyme exhibits a primary deuterium kinetic isotope effect of 2.0 and an inverse solvent deuterium isotope effect of 0.77 on V_2/K_{Lys}. A value of 2.0 was also observed for $^D(V_2/K_{Lys})_{D2O}$ when the primary deuterium kinetic isotope effect was repeated in D_2O, consistent with a rate-limiting hydride transfer step. A viscosity effect of 0.8 was observed on V_2/K_{Lys} indicating the solvent deuterium isotope effect resulted from stabilization of an enzyme form prior to hydride transfer. A small normal solvent isotope effect is observed on V, which decreases slightly when repeated with NADD, consistent with a contribution from product release to rate limitation. In addition, $V_2/K_{Lys}\mathbf{E_t}$ is pH independent consistent with the loss of an acid-base catalyst and perturbation of the pK_a of the second catalytic group to higher pH, likely a result of a change in the overall charge in the active site. The primary deuterium kinetic isotope effect for H96Q, measured in H_2O or D_2O, is within error equal to 1. A solvent deuterium isotope effect of 2.4 is observed with NADH or NADD as the dinucleotide substrate. Data suggest rate-limiting imine formation, consistent with the proposed role of H96 in protonating the leaving hydroxyl as the imine is formed. The pH-rate profile for $V_2/K_{Lys}\mathbf{E_t}$ exhibits the pK_a for K77, perturbed to a value of about 9, which must be unprotonated in order to accept a proton from the ε-amine of the substrate Lys so that it can act as a nucleophile. Overall,

*Corresponding authors: pcook@ou.edu, Tel: 405-325-4581, Fax: 405-325-6111, awest@ou.edu, Tel: 405-325-1529, Fax: 405-325-6111.

data are consistent with a role for K77 acting as the base that accepts a proton from the ε-amine of the substrate lysine prior to nucleophilic attack on the α-oxo group of α-ketoglutarate, and finally donating a proton to the imine nitrogen as it is reduced to give saccharopine. In addition, data indicate a role for H96 acting as a general acid-base catalyst in formation of the imine between the ε-amine of lysine and the α-oxo group of α-ketoglutarate.

Saccharopine dehydrogenase (N6-(glutaryl-2)-L-lysine: NAD oxidoreductase; EC 1.5.1.7) (SDH)[1] catalyzes the final step in the α-aminoadipate (AAA) pathway for the *de novo* synthesis of L-lysine in fungi (3, 4). The enzyme catalyzes the reversible pyridine nucleotide dependent oxidative deamination of saccharopine to generate α-Kg and Lys using NAD as an oxidant, Scheme 1 (3).

The proposed kinetic mechanism for the *Saccharomyces cerevisiae* SDH is ordered in the physiologic reaction direction with NAD binding before saccharopine (Sacc), while in the opposite direction α-ketoglutarate (α-Kg) and lysine (Lys) bind in random fashion once NADH is bound (5). A chemical mechanism involving two acid-base catalytic groups has been proposed on the basis of the pH dependence of kinetic parameters, Scheme 1 (6). Once the E•NADH•α-Kg•Lys central complex is formed, the first base (B_1) accepts a proton from the ε-amine of Lys to allow nucleophilic attack on the carbonyl of α-Kg (II). Nucleophilic attack gives a protonated carbinolamine with donation of a proton from the conjugate acid of B_2 to the carbonyl oxygen (III). The conjugate base of B_2 then accepts a proton from the carbinolamine nitrogen (IV) and this is followed by elimination of water to give the imine (V), which is reduced by NADH concomitant with protonation of the imine nitrogen by the conjugate acid of B_1. A number of residues (E78, E122, K99, D319) in the active site of SDH have been mutated and mutant enzymes have been characterized (7, 8). To date, none appear to serve as acid-base catalytic residues.

In this study the roles of K77 and H96 have been determined by mutating them to M and Q, respectively. Mutations of K77 and H96 were prepared in the C205S mutant enzyme, which eliminates disulfide formation, so that 100% of the enzyme is in the “reduced” active form (8). A 1.6 Å X-ray structure the apo-wild-type SDH enzyme was solved by the Berghuis group (9) and showed a tertiary fold consisting of two domains (I and II) with a narrow cleft in between. Each domain can be described as a modified nucleotide-binding Rossman-like fold. The active site is located at the bottom of the cleft between the two domains. Three additional X-ray structures have been solved of SDH bound to a sulfate anion, adenosine monophosphate (AMP), and oxalylglycine (OxGly), respectively (10). The sulfate-bound structure revealed features of how the α-keto acid substrate binds to R131 in the active site and showed a modest closure of the cleft between domains I and II. AMP was found to bind in the active site region expected to be occupied by the dinucleotide cofactor NAD. OxGly, an analogue of α-Kg, was observed to bind to two arginines, R18 and R131 in the active site. A semi-empirical model was proposed based on these ligand-bound structures with NAD and Sacc modeled in the active site.

We now report a crystal structure of the ternary E•NADH•Sacc complex for the first time, which shows an enzyme form with a closed active site with K77 and H96 properly positioned to serve as acid-base catalysts. Mutant enzymes were characterized via the pH

[1]Abbreviations: AAA, α-aminoadipate pathway; E, enzyme; SDH, saccharopine dehydrogenase; α-Kg, α-ketoglutarate; Sacc, L-saccharopine; Lys, L-lysine; NAD, β-nicotinamide adenine dinucleotide (the + charge is omitted for convenience); NADH, reduced β-nicotinamide adenine dinucleotide; NADD, reduced β-nicotinamide adenine dinucleotide with deuterium in the 4-R position; AMP, adenosine monophosphate; OxGly, oxalylglycine; WT, wild type; Mes, 2-(*N*-morpholino)ethanesulfonic acid; Taps, 3-[*N*-tris(hydroxymethyl) methylamino]-propanesulfonic acid; Hepes, *N*-(2-hydroxyethyl) piperazine-*N*’-(2-ethanesulfonic acid); Ches, 2-(*N*-cyclohexylamino) ethanesulfonic acid; PEG-MME, polyethylene glycol monomethyl ester; PKIE, primary kinetic isotope effects; SKIE, solvent kinetic isotope effects; MKIE, multiple kinetic isotope effects.

dependence of kinetic parameters and isotope effects. Data are discussed in terms of the proposed mechanism of SDH.

MATERIALS AND METHODS

Chemicals

Ampicillin, chloramphenicol, Sacc, Lys, α-Kg, AMP, OxGly, polyethylene glycol 3350, Bis-Tris propane, horse liver alcohol dehydrogenase, yeast aldehyde dehydrogenase, and the GenElute plasmid miniprep kit were obtained from Sigma. β-NADH, β-NAD, Luria-Bertani (LB) broth, LB-agar, and imidazole were purchased form U. S. Biochemical Corp. The buffers, Ches, Taps, Hepes, and Mes, were from Research Organics, while NiNTA resin was purchased from 5 Prime. Ethanol-d_6 (99 atom % D) and D_2O (99.9 atom % D) were purchased from Cambridge Isotope Laboratories. Ethanol (absolute, anhydrous) was from Pharmaco-Aaper. Polyethylene glycol monomethyl ether (PEG-MME) and Sodium Malonate were from Hampton Research. Isopropyl-β-D-1-thiogalactopyranoside was from Invitrogen. The QuikChange site-directed mutagenesis kit was from Stratagene, which includes PfuTurbo DNA polymerase and the *Dpn* I restriction enzyme. 4*R*-4-^{2}H NADH (NADD) was prepared as described previously (11). The concentration of NADD was estimated using an ε_{340} of 6220 $M^{-1}cm^{-1}$. All chemicals were obtained commercially, were of the highest grade available and were used without further purification.

Site-directed mutagenesis

Template DNA used for site-directed mutagenesis was the plasmid containing the C205S mutation of SDH, (1), to change K77 and H96 to M and Q, respectively. The forward and reverse primers used to generate the K77M mutant enzyme are as follows: $K77_f$, 5'-CATTATAGGTTTG**ATG**GAAATGCCTGAAACCG-3'; $K77_r$, 5'-CGGTTTCAGGCATTTC**CAT**CAAACCTATAA-3'. Primers used to generate the H96Q mutant enzyme are as follows: $H96_f$, CATCCAGTTTGCT**CAG**TGCTACAAAGACCAAGC-3'; $H96_r$, 5'-GCTTGGTCTTTGTAGCA**CTG**AGCAAACTGGATG-3'. In addition, a double mutant enzyme was prepared using the K77M forward and reverse primers and the H96Q mutant gene to generate K77M/H96Q. The mutated codon is shown in bold. PCR followed by mutagenesis was carried out according to the instructions in the QuikChange site-directed mutagenesis kit as described previously (7). The XL-1-Blue competent cell strain of *Escherichia coli* was transformed with the plasmids containing mutations. Plasmids were isolated and purified using the GenElute plasmid mini preparation kit (Sigma). Mutations were confirmed by sequencing the entire gene at the Sequencing Core of the Oklahoma Medical Research Foundation, Oklahoma City, OK.

Expression and purification

Escherichia coli BL21 (DE3)-RIL cells were transformed with plasmids containing mutant genes and expression was carried out as reported previously (5) with some modifications. Once cell density reached an A_{600} of 0.3–0.4, induction of protein expression was carried out at 37°C by addition of 0.2 mM IPTG, followed by 3-4 h incubation. Cells were harvested by centrifugation at 10,000*g* for 10 min, and then sonicated in 100 mM Hepes, pH 7.5, containing 300 mM NaCl, 5 mM imidazole. Enzymes were purified by Ni-NTA affinity chromatography, with elution using 300 mM imidazole. The enzymes were >95% pure as judged by SDS-PAGE. The enzymes were stored at 4°C in the elution buffer.

Enzyme assay

Initial velocities were measured using a Beckman DU 640 UV-visible spectrophotometer. All assays were performed at a temperature of 25°C. Enzyme activity was measured in quartz cuvettes with a path length of 1 cm in the direction of Sacc formation by monitoring the decrease in A_{340} (ε_{340} = 6220 M^{-1} cm^{-1}) as NADH is oxidized. When NADH had to be maintained at high concentrations the reaction was monitored at 366 nm (ε_{366} = 3110 M^{-1} cm^{-1}) using a path length of 0.4 cm. Reactions were initiated by addition of enzyme to a reaction mixture with a final volume of 0.5 mL containing 100 mM Hepes, pH 7.0, saturating NADH (0.5 mM) and variable concentrations of α-Kg and Lys.

pH studies

The pH dependence of V, V/K_{Lys}, and $V/K_{\alpha\text{-}Kg}$ was measured over the pH range 5–10 with NADH maintained at 0.5 mM, and either α-Kg or Lys maintained at saturation with the other varied. Buffers were maintained at 100 mM concentration in the following pH range; Mes, 5.5 - 7.0; Hepes, 7.0 - 8.0; Taps, 8.0 - 9.0; Ches, 9.0 – 10.0. None of the buffers had any effect on the activity of any of the mutant enzymes. The pH was recorded before and immediately after the reaction; no significant differences were detected. To be certain that the kinetic mechanism of the enzyme did not change with pH and to obtain estimates of K_m values for both substrates at the pH extremes, initial velocity patterns were obtained at extreme pH values (5.5 and 10.0) with α-Kg and Lys concentrations varied, and NADH was maintained at a saturating concentration (0.5 mM).

Kinetic isotope effects

Isotope effects were measured for K77M and H96Q mutant enzymes in the pH independent region of their pH-rate profiles (pH 9). Isotope effects on V_2 and V_2/K_{Lys} were measured with NADH(D) ($10K_m$) and α-Kg ($10K_m$) maintained at saturation and Lys varied. Solvent deuterium kinetic isotope effects were measured at pH(D) 9, in the pH independent region of the pH(D)-rate profiles. For rates measured in D_2O, substrates (α-Kg and Lys) and buffers were first dissolved in a small amount of D_2O and then lyophilized to replace exchangeable protons. The lyophilized powders were then re-dissolved in D_2O to give the desired concentrations, and pD was adjusted using either DCl or NaOD. NADH was dissolved in D_2O directly. Reactions were initiated by adding a small amount of each of the mutant enzymes in H_2O; the final concentration of D_2O in the reaction mixture was about 98%. Multiple isotope effects were determined by direct comparison of the initial rates in H_2O and D_2O as for solvent deuterium effects, varying lysine at fixed saturating concentration of NADD and α-Kg.

Viscosity effects

Initial velocities were determined in H_2O at a relative viscosity of 1.24 at pH 8.0 and 25°C. Assays contained 9% glycerol (w/v) as the viscosogen, which generates the same relative viscosity as 100% D_2O at 25 °C (12). The effect of viscosity on V and V/K ($^{\eta}V$ and $^{\eta}(V/K)$) were determined as the ratio of V and V/K in the absence and presence of glycerol.

Data Analysis

Initial rate data were first analyzed graphically by double reciprocal plots to determine the quality of the data and the proper rate equation for data fitting. Data were then fitted using the appropriate equations (2) using the Marquardt-Levenberg algorithm (13), supplied with the EnzFitter program from BIOSOFT, Cambridge, U.K. Kinetic parameters and their corresponding standard errors were estimated using a simple weighing method.

Data from saturation curves for pH-rate profiles and viscosity effects were fitted to eq. 1. Data obtained from the initial velocity patterns were fitted to eq. 2. Data for *V* and *V/K* deuterium isotope effects were fitted using eqs. 3 and 4. Equal isotope effects on *V* and *V/K* are assumed in eq. 3, while the isotope effects on *V* and *V/K* are allowed to be independent in eq. 4. The S.E. of a product or dividend was estimated using eq. 5.

$$v=\frac{V\mathbf{A}}{K_a+\mathbf{A}} \tag{1}$$

$$v=\frac{V\mathbf{AB}}{K_{ia}K_b+K_a\mathbf{B}+K_b\mathbf{A}+\mathbf{AB}} \tag{2}$$

$$v=\frac{V\mathbf{A}}{(K_a+\mathbf{A})\,(1+F_iE_v)} \tag{3}$$

$$v=\frac{V\mathbf{A}}{K_a\left(1+F_iE_{V/K}\right)+\mathbf{A}\,(1+F_iE_V)} \tag{4}$$

$$\text{S.E.}\frac{x}{y}=\frac{x}{y}\left[\left(\frac{\text{S.E.}x}{x}\right)^2+\left(\frac{\text{S.E.}y}{y}\right)^2\right]^{1/2} \tag{5}$$

In eqs. 1-4, *v* and *V* are initial and maximum velocities, respectively, **A, B**, are substrate concentrations, K_a and K_b, are Michaelis constants for substrates A and B, respectively, and K_{ia} is the dissociation constant for A from the EA complex. In eqs. 3 and 4, F_i is the fraction of label in substrate or solvent, E_v, E_V and $E_{V/K}$ are isotope effects minus 1 for the equal isotope effects on *V* and *V/K*, and the independent isotope effects on *V* and *V/K*, respectively. In eq. 5, S.E. *x*, and S.E. *y* are computer generated standard errors of values for kinetic parameters *x* and *y*.

Data for pH-rate profiles exhibiting a partial change on the acid side were fitted to eq. 6.

$$\log y=\log\left[Y_L+Y_H\left(\frac{\mathbf{H}}{K_1}\right)/\left(1+\frac{\mathbf{H}}{K_1}\right)\right] \tag{6}$$

In eq. 6, *y* is the observed value of *V* or *V/K* at any pH, **H** is the hydrogen ion concentration, K_1 is the acid dissociation constant of functional group required in a given protonation state on enzyme or substrate for optimal binding and/or catalysis, and Y_L and Y_H are pH-independent constant values of *y* at low and high pH, respectively.

Crystallization

The purified SDH C205S mutant enzyme was crystallized based on fine screening of the conditions described by Andi *et al*. (10) for the apo-SDH wild-type enzyme. The final reservoir conditions for crystallization of the SDH C205S enzyme were 100 mM Tris (pH 7.0), 30% (w/v) PEG-MME 2000 at 4 °C using the hanging drop vapor diffusion method. The hanging drop contained equal volumes of protein (14-18 mg/mL in 0.1 M Hepes, pH 7.0) and reservoir solution (2 μl each). Trays were cooled and setup at 4 °C.

Diffraction quality crystals could not be obtained by soaking Sacc and NADH into the apo-C205S SDH crystals. Likewise, co-crystallization trials with the SDH C205S enzyme with Sacc and NADH using the original apo-SDH conditions did not produce diffraction quality crystals. New co-crystallization conditions were found based on broad screen crystallization trials carried out using the Mosquito liquid handler from TTP Labtech. A series of optimization screens were developed by varying the concentrations of polyethylene glycol (PEG) 3350 from 10 – 25 % w/v, malonate from 0 – 0.3 M with 0.1 M Bis-Tris Propane (pH 6.5). Trials were set up in 24 well VDX crystallization plates using a Rigaku Automation Alchemist II liquid handler. The final conditions that yielded diffraction quality crystals of the E•Sacc•NADH complex were 22% PEG 3350, 0.3 M malonate and 0.1 M Bis-Tris Propane (pH 6.5) at 4 °C.

X-ray data collection

All data was collected at 100 K and crystals were cryo-protected by transfer through increasing concentrations of glycerol to a final concentration of 15%. All crystals were rapidly cryo-cooled in liquid nitrogen.

X-ray data for the C205S apo-enzyme and E•Sacc•NADH complex crystals were collected at 100 K using CuKα (λ = 1.5418 Å) radiation on a Rigaku RU3HR rotating anode generator and RAXIS IV^{++} image plate detector. Diffraction data were integrated using Mosflm, scaled and merged using SCALA and structure factors were calculated using TRUNCATE as found in the CCP4 program suite (14). Data collection statistics are given in Table 1.

Molecular replacement

Initial phasing for both structures was done by molecular replacement using PHASER (15) The native apo-enzyme structure (PDB ID: 2Q99) was used as the initial search model for the apo-C205S structure (9). The resultant C205S structure was used as a search model in molecular replacement to solve the E•Sacc•NADH structure. There is a significant conformational change that occurs upon Sacc/NADH binding, and as a result the apo-enzyme model had to be edited by separating it into two halves at residues Phe135 and Pro326. Refinement was conducted using REFMAC (16), with a round of simulated annealing done initially in PHENIX (17) to reduce model bias. Model visualization, rebuilding and the fitting of Sacc and NADH were done using COOT (18). Water molecules were added toward the end of refinement using the Add Waters function in COOT and visually inspected after initial placement. A glycerol molecule was also found in the ligand bound structure. Refinement statistics are given in Table 1.

Molecular graphics

Structure figures were prepared using *PyMOL*™ version 1.2b6pre (19).

RESULTS

Cell growth, expression and purification

Expression of the K77M/C205S, H96Q/C205S and K77M/H96Q/C205S mutant enzymes was similar to that of the WT SDH. All enzymes eluted from the Ni-NTA column with buffer containing 300 mM imidazole at pH 8. Purity of the proteins was assessed by SDS-PAGE, and all of the mutant proteins were estimated to be >95% pure. The His-tagged mutant enzymes maintained stability and remained active for months when stored at 4 °C in 100 mM Hepes, 300 mM KCl, and 300 mM Imidazole at pH 8.

Structural studies

The X-ray structure of the pseudo-WT C205S apo-enzyme (PDB ID code: 3UGK) was solved from crystals grown as described in **MATERIALS AND METHODS**. Diffraction data indicated a space group of $P2_12_12_1$ and the highest resolution shell was 2.01 Å, Table 1. The structure was solved by molecular replacement and initially built from the SDH model (PDB ID 2Q99) published by Berghuis and colleagues (9). The structure of the C205S apo-enzyme is virtually identical to that of the WT enzyme. A superimposition of the two structures gives an rmsd of 0.31 Å (data not shown).

Attempts to crystallize a ternary complex of the WT enzyme were unsuccessful, likely as a result of very weak binding of the cofactor to enzyme with an oxidized disulfide (5). A ternary complex structure was obtained by co-crystallization of the C205S enzyme with Sacc and NADH (PDB ID code: 3UH1). Diffraction data indicated a space group of $P4_3$ and the highest resolution shell was 2.17 Å, Table 1. The structure was solved by molecular replacement using the structure of the apo-C205S enzyme as discussed in **MATERIALS AND METHODS**. A superimposition of the E•Sacc•NADH ternary complex structure with the apo-C205S structure indicated significant changes that result in a closure of the active site, Figure 1A. In the ternary complex, there is a slight rotation and rigid body movement of almost 9 Å of domain I towards domain II that effectively closes the cleft region as shown in the CPK models in Figure 1B (apo) versus Figure 1C (ternary complex). The net displacement of K99 in the C97-K103 loop region is 8.8 Å in the ternary complex relative to the apo-enzyme.

Figure 2A shows a stereoview of an F_o-F_c difference electron density map of the active site region to illustrate the positions of the bound NADH and Sacc molecules. Figure 2B is a monoview of the active site with hydrogen bond and ionic interactions shown for protein side chains in contact with the ligands. The distances between enzyme side chain atoms and reactants are given in Table 4. The Nε atom of K77 and the Nε2 atom of H96 form hydrogen bonds with the Nε atom of Sacc. Other important contacts are made through R18, E122. Also shown is an ionic interaction between D227 and NADH. There are several hydrogen-bond interactions between the cofactor NADH and the substrate saccharopine.

We also attempted to co-crystallize SDH with NADH and lysine using the same screening conditions as for the E•Sacc•NADH ternary complex crystals. However, we only observed density for NADH in the solved structure (PDB ID: 3UHA) and the enzyme was observed to be in the open conformation (data not shown).

Initial velocity studies

Initial velocities were measured in the direction of Sacc formation for the K77M, H96Q and K77M/H96Q mutant enzymes. Replacing K77 with M resulted in a 145-fold decrease in $V_2/\mathbf{E_t}$ and $>10^4$-, and $>10^3$-fold decreases in $V_2/K_{\alpha\text{-}Kg}\mathbf{E_t}$ and $V_2/K_{Lys}\mathbf{E_t}$, respectively. This results in 28- and 90-fold increases in K_{Lys} and $K_{\alpha\text{-}Kg}$, respectively. Replacing H96 with Q resulted in a 28-fold decrease in $V_2/\mathbf{E_t}$ and $>10^3$-fold decreases in $V_2/K_{\alpha\text{-}Kg}\mathbf{E_t}$ and $V_2/K_{Lys}\mathbf{E_t}$, respectively. The $K_{\alpha\text{-}Kg}$ and K_{Lys} increased 80-, and 300-fold, respectively. The K77M/H96Q double mutant gave the largest changes in kinetic parameters, as expected, with 660-, $>10^6$-, and $\sim10^5$-fold decreases in $V_2/\mathbf{E_t}$, $V_2/K_{\alpha\text{-}Kg}\mathbf{E_t}$, and $V_2/K_{Lys}\mathbf{E_t}$, respectively; $K_{\alpha\text{-}Kg}$ and K_{Lys} increased $>10^3$- and 10^2-fold, respectively. Kinetic parameters are summarized in Table 2, and compared to those obtained for the pseudo-WT, C205S (1).

pH dependence of kinetic parameters

The pH dependence of kinetic parameters provides information on the optimal protonation state of functional groups on enzyme and/or substrate for binding and/or catalysis. Studies

were carried out with K77M and H96Q mutant enzymes in the direction of saccharopine formation, at 25 °C; the rate obtained with the double mutant enzyme were too low to allow data to be collected as a function of pH. Both mutant enzymes were active and stable over the pH range 5–10, and initial rate studies at pH 5.5 and 10 suggest the kinetic mechanism did not change (data not shown). For the K77M mutant enzyme, $V_2/K_{Lys}\mathbf{E_t}$ is pH independent, while $V_2/\mathbf{E_t}$ exhibits a partial change on the acid side giving a pK_a of about 7.4. pH independent values of $V_2/\mathbf{E_t}$ are 0.20 ± 0.03 s^{-1} at low pH and 1.4 ± 0.1 s^{-1} at high pH. The average pH independent value of $V_2/K_{Lys}E_t$ is 0.8 ± 0.5. In the case of H96Q, $V_2/\mathbf{E_t}$ exhibits a decrease at low pH with a slope <1, giving an app pK_a of about 6.7, while $V_2/K_{Lys}E_t$ exhibits a partial change with a pK_a of about 9, decreasing from a constant value at high pH to a lower constant value at low pH. The pH independent value of $V_2/\mathbf{E_t}$ is 4.8 ± 0.3 s^{-1}, while values of 450 ± 280 and 4.5 ± 2.9 $M^{-1}s^{-1}$ are obtained for $V_2/K_{Lys}E_t$ at high and low pH, respectively.

Isotope effects

Isotope effects were measured for the K77M mutant enzyme at pH 9, the high pH independent region of the pH-rate profiles. Values of 1.8 and 2.0 were obtained for $^{D}V_2$ and $^{D}(V_2/K_{Lys})$, and both are greater than the value of 1.3 reported for the pseudo-WT enzyme (C205S). A small normal ^{D2O}V is observed, but $^{D2O}(V/K_{Lys})$ is inverse. Repeating the solvent effect with NADD gave only slight changes. On the other hand, a repeat of the primary deuterium effect in D_2O gives a decrease in the isotope effect on V from 1.8 to 1.4, but no change in the isotope effect on V_2/K_{Lys}.

For H96Q, the primary deuterium isotope effect is within error unity, whether measured in H_2O or D_2O. The solvent deuterium kinetic isotope effect is 2.4 and there is no significant change when it is measured with NADD. Data are summarized in Table 3, and compared to those obtained for C205S mutant enzyme (1).

Viscosity effects

In order to determine whether the SKIEs reflect the increased viscosity in D_2O, the initial rate was measured in the absence and presence of 9% glycerol, which gives a relative viscosity of 1.24, the same as 100% D_2O (20). There was no effect of viscosity on V and V/K for the H96Q mutant enzyme; a value of 1.02 ± 0.01 was obtained. For K77M, $^{\eta}V$ and $^{\eta}(V/K)$ were 1.18 ± 0.03 and 0.61 ± 0.06.

DISCUSSION

Structures

Previous structures of apo-wild type SDH (9) and substrate analogue bound structures (10) showed an open or partially closed cleft between domains I and II. The E•NADH•Sacc ternary complex structure described here reveals a closed conformation in which reactants are tightly bound to the enzyme via hydrogen bond and ionic interactions and poised for acid-base catalysis. A slight rotation and 8.8 Å shift of domain I towards domain II is responsible for closing the active site.

On the basis of the ternary E•NADH•Sacc complex of SDH, there are a number of ionizable residues in the active site as discussed in the Introduction. Residues include R18, R131, K99, K77, K13, E122, E78, E16, and H96. A multiple sequence alignment of the SDH from *Saccharomyces cerevisiae*, *Candida albicans*, *Aspergillus fumigatus*, *Cryptococcus neoformans*, *Magnaporthe grisea*, *Yarrowia lipolytica* and *Schizosaccharomyces pombe* indicated that all of these active site residues are conserved in these fungal species (data not shown), consistent with their importance in the mechanism.

As shown in Figure 2A, K77 and H96 are within hydrogen-bond distance (3.4 Å and 3.5 Å, respectively) to the secondary amine of saccharopine, and could serve as acid-base catalysts in the dehydrogenase reaction. The proposed mechanism suggests that one of the residues accepts a proton from the secondary amine in the hydride transfer step, while the second activates water for hydrolysis of the resulting imine. The lysine and imidazole side chains of K77 and H96 are in proper position to carry out these functions. Data presented in Results above are in agreement with this hypothesis and further discussed below.

Kinetic parameters

All three mutant enzymes, K77M, H96Q, and K77M/H96Q, were characterized in the direction of Sacc formation. Initial rates measured as a function of reactant concentration suggested the kinetic mechanism did not change compared to that proposed for the C205S pseudo-WT enzyme, i. e., binding of NADH first, followed by random addition of α-Kg or Lys (data not shown).

Mutating K77 to M decreases the positive charge in the site, while changing H96 to Q likely does not change the overall charge assuming the imidazole side chain is neutral at neutral pH. Mutation of K77 gives a 145-fold decrease in V/E_t, the largest thus far observed for any site-directed mutation in SDH (7, 8). The two order of magnitude decrease in the turnover number and 3 to 4 order of magnitude decreases in the second order rate constants are consistent with the K77 side chain playing a direct role as an acid-base catalyst in the SDH reaction. Substitution of a glutamine for H96 leads to a 28-fold decrease in the turnover number of SDH and greater than 3 order of magnitude decreases in second order rate constants. Although the decreases are not as great as those observed for the K77M mutant enzyme, the data are suggestive of a catalytic role for H96. In agreement, the double mutant enzyme, K77M/H96Q, gives a nearly 3 order of magnitude decrease in $V_2/\mathbf{E_t}$ and 5 to 6 order of magnitude decreases in the second order rate constants. These data, together with the position of the two residues in the site are consistent with their role as acid-base catalysts in the reaction.

Isotope effects

Primary and solvent isotope effects are sensitive tools to investigate the slow step / rate determining steps in the reaction. The primary deuterium kinetic isotope effect (PKIE) reflects the hydride transfer step (see Scheme 1) (6). A solvent kinetic isotope effect (SKIE) is observed when protons are in flight in transition states that contribute to rate limitation. In the WT and C205S enzymes, the SKIE was derived from protons in flight in the hydride transfer and imine hydrolysis steps, corroborated by a concave downward proton inventory (6).

The maximum rate for the C205S mutant enzyme is slightly pH dependent decreasing from a constant value at high pH to another constant value at low pH. The isotope effects for the C205S enzyme reported in Table 3 were measured at pH 9 (1). The effects obtained at pH 5.6 are about 2, similar to the value obtained for the K77M mutant at pH 9. The data suggest hydride transfer is slower for the K77M mutant enzyme. The slightly lower isotope effect on V suggests release of NAD or isomerization of the E-NADH complex contributed to rate limitation. The SKIE on V is similar to that obtained for C205S, but the effect on V/K_{Lys} is unexpectedly inverse, and will be discussed further below. A repeat of the PKIE in D_2O gives a value of $^{D}(V/K_{Lys})$ equal to that obtained in H_2O suggesting that the hydride transfer step is rate-determining at pH 9, and the observed solvent deuterium isotope effect reflects changes that occur or have occurred once the transition state for hydride transfer is attained. The PKIE on V in D_2O decreases slightly consistent with a step in addition to hydride transfer contributing to rate limitation; the data are consistent with the suggestion that

release of NAD or isomerization of the E-NADH complex contributed to rate limitation. A repeat of the SKIE with NADD fixed gives values that are either identical to or decreased slightly compared to the value in H_2O. Taken together, the data indicate hydride transfer as the step that is largely rate-determining at limiting Lys (V/K_{Lys}), and is a major contributor to rate limitation at saturating reactant concentrations. Thus, as suggested on the basis of structural studies and pH-rate profiles (see below) K77 is, in all likelihood, the base that donates a proton to the secondary amine of Sacc in the hydride transfer step as the imine is reduced.

Inverse SKIEs are expected for ionization of a thiol, hydrolysis of metal-H_2O, a medium effect (20), or an effect derived from the increase in viscosity generated by D_2O. Although there is a thiol in the vicinity of the dinucleotide-binding site, it is unlikely this ionization contributes to the chemistry in the site. If anything it would be expected to decrease the affinity of enzyme for NADH, and this is not observed. There is no metal ion involved in the SDH reaction. It is thus possible that either a medium effect or an effect of viscosity is responsible for the observed inverse SKIE, and may reflect the conformational change to close the site to form the productive Michaelis complex upon binding of Lys. The viscosity effect is identical to the measured SKIE, consistent with a preference for the closed conformation because of the higher viscosity of D_2O.

The solvent isotope effects, listed in Table 3, are nearly identical to the viscosity effects obtained for K77M. Data strongly suggest the inverse isotope effect on *V/K* is a consequence of the change in solvent viscosity in D_2O, i.e., the solvent deuterium isotope effect on *V/K* is 1.0, while a slight normal isotope effect of about 1.23 ± 0.02 (1.45/1.18) is observed on *V*. Effects near unity suggest proton transfer steps do not contribute or contribute to a very small extent to the rate limitation in the reaction with Lys limiting. The reason for the increased rate in the presence of a viscosogen is not known at this point but likely results from stabilization of an enzyme conformation along the reaction pathway as suggested above. At saturating reactant concentrations, there is a slight contribution from diffusion (viscosity effect) and there is at least one proton in flight in a step that contributes to rate limitation. As suggested above, the step reflects either release of NAD or isomerization of the E•NADH complex, and the presence of a contribution from diffusion suggests that it is likely release of NAD.

Observation of an inverse viscosity effect is not unique to SDH. Similar observations have been made for the *Ascaris suum* NAD malic enzyme (20), and the homoisocitrate dehydrogenase from *S. cerevisiae* (21) using 9% glycerol as the viscosogen. Inverse solvent deuterium isotope effects and viscosity effects of about 0.8 and 0.5 were estimated on *V* and V/K_{malate} for the malic enzyme. These results, with a larger inverse effect on *V/K* than *V,* are qualitatively identical to those obtained in these studies. Data were interpreted in terms of stabilizing the closed form of the enzyme at higher viscosity. The increase in rate is thus a result of an increase in the concentration of the productive Michaelis complex. Isocitrate, a slow substrate for homoisocitrate dehydrogenase, also gave similar inverse solvent isotope and viscosity effects of 0.8 and 0.6 on *V* and V/K_{Ic}. Data were again interpreted in terms of stabilizing an enzyme form along the reaction pathway.

Isotope effects measured for H96Q are very straightforward and easy to interpret. A primary deuterium effect near 1 indicates the hydride transfer step does not contribute to rate limitation. The SKIE is about 2.3 on *V* and V/K_{Lys}, significantly greater than the value obtained for C205S. Data are consistent with the proposed role of H96 in formation of the imine prior to its reduction in the hydride transfer step.

pH dependence of kinetic parameters

To further probe the role of K77 and H96, the pH dependence of kinetic parameters was measured. These studies allow a determination of the optimal protonation state of the functional groups on the enzyme and/or substrate involved in either binding and/or catalysis. On the basis of the above discussion, the proposed general base in the direction of Sacc formation is K77, which must accept a proton from the ε-amine of Lys as it attacks the α-carbonyl of α-Kg to form the imine. Histidine 96 is proposed to serve a role as a general acid in the reaction, first protonating the carbonyl oxygen to form the protonated carbinolamine, accepting a proton from the protonated carbinolamine to generate the neutral carbinolamine, and eventually protonating the leaving hydroxide to give water (III in Scheme I).

Data for the C205S mutant enzyme (1) are shown in Fig. 3 as a reference for interpreting the pH-rate profiles for K77M and H96Q. V_2 decreases from a constant value at low pH to a lower constant value at high pH. The pK_a estimated for the change is 7.5 and the ratio of the constant values is about 9. The pH dependence was attributed to a conformational change in enzyme, with the low pH conformation the more active of the two. (This aspect will be discussed further below.) The *V/K* for Lys exhibits a bell-shaped pH-rate profile with pK_a values of 7 and 8.1 attributed to the general base and general acid in the SDH reaction.

Data for the K77M mutant enzyme differ considerably. The V_2 pH-rate profile exhibits a partial change, but requires the group unprotonated, opposite the situation for C205S. It is clear that the presence of the K77 side chain influences the pK_a and perhaps the group responsible for pH-dependent conformational change. On the basis of the isotope effects presented in **RESULTS** and discussed above, the hydride transfer step is slow for the K77M mutant enzyme, and we propose that K77 donates a proton as the imine is reduced to the secondary amine in Sacc. The loss of the side chain of K77 results in a significant decrease in the rate at low pH, which increases with increasing pH giving a pK_a of about 7.5. The data obtained in these studies suggest an interpretation that is alternative to a pH dependent conformational change. Although chemistry contributes to rate limitation for the pseudo-WT enzyme, the conformational changes required to close the site prior to catalysis and open it prior to product release also make significant contributions (5, 8). The pH dependence observed in the V_2 pH-rate profile may reflect two pathways that differ depending on the protonation state of the ε-amino groups of the Lys substrate and the side chain of K77. For the C205S mutant enzyme, the optimum protonation state exists when the substrate ε-amine is protonated and the side chain of K77 is unprotonated. The proximity of the side chain of Lys and K77, results in a decrease in the pK_a of both ε-amino groups facilitating proton transfer from one to the other. As the pH increases, the proton shared between the two side chains is lost; the global pK_a is about 7.5 for the Lys-K77 pair on the basis of the observed pK_a values. Once unprotonated, the rate decreases by 9-fold, likely as a result of a change in orientation of the Lys side chain. In the K77M mutant enzyme the protonation state of the substrate Lys ε-amine may also contribute to rate limitation at saturating reactants. Once bound the Lys ε-amine must be unprotonated to act as a nucleophile as it attacks the α-carbonyl of α-Kg to form the imine. Other active site side chains, e.g., E78, E16, or K13, must abstract the Lys ε-amine proton, perhaps via the intermediacy of a water molecule. As the pH increases the ε-amine of Lys becomes unprotonated (the pK_a is around 7.5 for the bound substrate), can serve as a nucleophile, and the rate increases by about 10-fold.

The dominant forms of enzyme and substrate present when V/K_{Lys} is measured is the E•NADH•α-Kg complex and free Lys. The V/K_{Lys} is pH independent, while a bell-shaped pH-rate profile was obtained for C205S with pK_a values of about 7 and 8. Since free Lys is dominant, the observed pK_as are on enzyme; the pK_a of the α- and ε-amino groups of Lys are 9.5 and 10.5, respectively. One of the pK_a values likely reflects the K77 side chain, and intrinsic values are observed.[2] It is likely the group with a p*K* of about 7 that reflects the

K77 side chain, consistent with the discussion of the pK_a of 7.5 in the $V_2/\mathbf{E_t}$ pH-rate profile above. The pK_a of the H96 side chain is thus about 8 and in the absence of the K77 side chain is perturbed to a pH higher than 9.5, perhaps resulting from the influence of E78, which is in the vicinity and no longer neutralized by K77. The absence of the pK_a of about 7 is consistent with its attribution to K77.

In the case of the H96Q mutant enzyme, interpretation will begin with the V/K_{Lys} pH-rate profile. Note that the profile exhibits a partial change, decreasing from a constant value above pH 9 to a lower constant value below pH 6; the ratio of the constant values is about 100. The observed pK_a of about 9 reflects the side chain of K77, while the pK_a observed at high pH in C205S is absent consistent with assignment of H96 as this group. The loss of the H96 side chain resulted in an increase in the pK_a of K77 from about 7.5 to 9, suggesting an influence of the imidazole side chain on the proton affinity of the K77 side chain. The H96 side chain must be protonated for optimum reaction in the direction of Sacc formation, and the proximity of the positive charge on the imidazole will certainly result in a decrease in the pK_a of the ε-amino groups of K77. The finite rate obtained at low pH suggests K77 is important for catalysis, but is not absolutely essential. This is in agreement with the data obtained for the $V_2/\mathbf{E_t}$ pH-rate profiles for C205S, K77M and H96Q (see below).

The $V_2/\mathbf{E_t}$ pH-rate profile of H96 is similar to that of K77M at face value. However, since the K77 side chain is absent the pK_a reflected is that of the bound substrate, Lys. Thus, the bound Lys has a pK_a of about 7. As the pH increases and the ε-amino of bound Lys becomes neutral, the rate increases since the amine can now act as a nucleophile in the attack of the α-carbonyl of α-Kg to form the imine.

Conclusions

A structure of a ternary complex between the C205S pseudo-WT enzyme, NADH, and Sacc provided a closed form of the enzyme and a more accurate description of the interactions between enzyme side chains and reactant functional groups compared to the semi-empirical model published previously (10). Importantly, the distance between C4 of the nicotinamide ring to C8 of Sacc is 3.6 Å as shown in Figure 2, a reasonable hydride transfer distance, compared to a distance of >4.5 Å estimated from the semi-empirical model (10), which was constructed from open forms of the enzyme. The side chains of H96 and K77 now appear properly positioned to act as acid-base catalysts.

Mutation of K77 to M results in 145-fold decrease in $V/\mathbf{E_t}$ and greater than three order of magnitude increase in the second order rate constants. Together with the large primary deuterium isotope effect (2.0) and small solvent deuterium isotope effect (1.45), data suggest rate limiting hydride transfer, consistent with the proposed general acid role of K77 in protonating the imine nitrogen concomitant with hydride transfer. In agreement with this proposal, $V_2/K_{Lys}\mathbf{E_t}$ is pH independent. The H96Q mutation, results in about a 28-fold decrease in $V_2/\mathbf{E_t}$ and $>10^3$-fold decreases in the second order rate constant. A primary deuterium isotope effect near unity and a large solvent deuterium isotope effect (2.4) is consistent with the proposed role of H96 in protonating the leaving hydroxyl as the imine is formed. Elimination of H96 results in a pH-rate profile for $V_2/K_{Lys}\mathbf{E_t}$ that exhibits the pK_a for K77, which must be unprotonated in order to accept a proton from the ε-amine of the substrate Lys so that it can act as a nucleophile. The proposed roles of H96 and K77 are corroborated by the nearly 700-fold decrease in $V_2/\mathbf{E_t}$ and $>10^5$-fold decreases in the second order rate constants.

[2]A partial change was observed in the $V_2/\mathbf{E_t}$ pH-rate profile of C205S, which was proposed to reflect a pH dependent conformational change (1). pK_as for the catalytic groups are not observed suggesting optimum binding of only the correctly protonated forms of reactants and enzyme. In this case, intrinsic pK_a values are observed (2).

Acknowledgments

This work was supported by a grant (GM 071417) from the National Institutes of Health and the Grayce B. Kerr Endowment to the University of Oklahoma to support the research of P.F.C.

References

1. Bobyk KD, Kim SG, Kumar VP, Kim SK, West AH, Cook PF. The oxidation state of active site thiols determines activity of saccharopine dehydrogenase at low pH. Arch Biochem Biophys. 2011; 513:71–80. [PubMed: 21798231]
2. Cook, PF.; C, WW. Enzyme kinetics and mechanism. Taylor & Francis Group, LLC; New York: 2007.
3. Xu H, Andi B, Qian J, West AH, Cook PF. The α-aminoadipate pathway for lysine biosynthesis in fungi. Cell Biochem Biophys. 46:43–64. [PubMed: 16943623]
4. Zabriskie TM, Jackson MD. Lysine biosynthesis and metabolism in fungi. Nat Prod Rep. 2000; 17:85–97. [PubMed: 10714900]
5. Xu H, West AH, Cook PF. Overall Kinetic Mechanism of Saccharopine Dehydrogenase from *Saccharomyces cerevisiae*. Biochemistry. 2006; 45:12156–12166. [PubMed: 17002315]
6. Xu H, Alguindigue SS, West AH, Cook PF. A proposed proton shuttle mechanism for saccharopine dehydrogenase from *Saccharomyces cerevisiae*. Biochemistry. 2007; 46:871–882. [PubMed: 17223709]
7. Ekanayake DK, Andi B, Bobyk KD, West AH, Cook PF. Glutamates 78 and 122 in the active site of saccharopine dehydrogenase contribute to reactant binding and modulate the basicity of the acid-base catalysts. J Biol Chem. 2010; 285:20756–20768. [PubMed: 20427272]
8. Ekanayake DK, West AH, Cook PF. Contribution of K99 and D319 to substrate binding and catalysis in the saccharopine dehydrogenase reaction. Arch Biochem Biophys. 2011; 514:8–15. [PubMed: 21819960]
9. Burk DL, Hwang J, Kwok E, Marrone L, Goodfellow V, Dmitrienko GI, Berghuis AM. Structural studies of the final enzyme in the α-aminoadipate pathway-saccharopine dehydrogenase from *Saccharomyces cerevisiae*. J Mol Biol. 2007; 373:745–754. [PubMed: 17854830]
10. Andi B, Xu H, Cook PF, West AH. Crystal Structures of Ligand-Bound Saccharopine Dehydrogenase from *Saccharomyces cerevisiae*. Biochemistry. 2007; 46:12512–12521. [PubMed: 17939687]
11. Viola RE, Cook PF, Cleland WW. Stereoselective preparation of deuterated reduced nicotinamide adenine nucleotides and substrates by enzymatic synthesis. Anal Biochem. 1979; 96:334–340. [PubMed: 224725]
12. Quinn, DM.; S, LD. Enzyme mechanism from isotope effects. CRC Press; Boca Raton, FL: 1991.
13. Marquardt DW. An algorithm for least square estimation of nonlinear parameters. J Soc Ind Appl Math. 1963; 11:431–441.
14. Winn M, Ballard CC, Cowtan KD, Dodson EJ, Emsley P, Evans PR, Keegan RM, Krissinel EB, Leslie AGW, McCoy A, McNicholas SJ, Murshudov GN, Pannu NS, Potterton EA, Powell HR, Read RJ, Vagin A, Wilson KS. Overview of the CCP4 suite and current developments. Acta Cryst. 2011; D67:235–242.
15. McCoy AJ, Grosse-Kunstleve RW, Adams PD, Winn MD, Storoni LC, Read RJ. Phaser crystallographic software. J Appl Cryst. 2007; 40:658–674. [PubMed: 19461840]
16. Murshudov GN, Skubak P, Lebedev AA, Pannu NS, Steiner RA, Nicholls RA, Winn MD, Long F, Vagin AA. REFMAC5 for the refinement of macromolecular crystal structures. Acta Cryst. 2011; D67:355–367.
17. Adams PD, Afonine PV, Bunkoczi G, Chen VB, Davis IW, Echols N, Headd JJ, Hung L-W, Kapral GJ, Grosse-Kunstleve RW, McCoy AJ, Moriarty NW, Oeffner R, Read RJ, Richardson DC, Richardson JS, Terwilliger TC, Zwart PH. PHENIX: a comprehensive Python-based system for macromolecular structure solution. Acta Cryst. 2010; D66:213–221.
18. Emsley, Pa; C, K. Coot: model-building tools for molecular graphics. Acta Cryst. 2004; D 60:2126–2132.

19. Delano, WL. The PyMOL molecular graphics system. San Carlos, CA: Delano Scientific; 2004.

20. Karsten WE, L CJ, Cook PF. Inverse solvent isotope effects in the NADmalic enzyme reaction are the result of the viscosity difference between D2O and H2O: Implications for solvent isotope effect studies. J Am Chem SOC. 1995; 117:5914–5918.

21. Lin Y, Volkman J, Nicholas KM, Yamamoto T, Eguchi T, Nimmo SL, West AH, Cook PF. Chemical Mechanism of Homoisocitrate Dehydrogenase from *Saccharomyces cerevisiae*. Biochemistry. 2008; 47:4169–4180. [PubMed: 18321070]

22. Chen VB, Arendall WB III, Headd JJ, Keedy DA, Immormino RM, Kapral GJ, Murry LW, Richardson JS, Richardson DC. MolProbity: all-atom structure validation for macromolecular crystallography. Acta Cryst. 2010; D66:12–21.

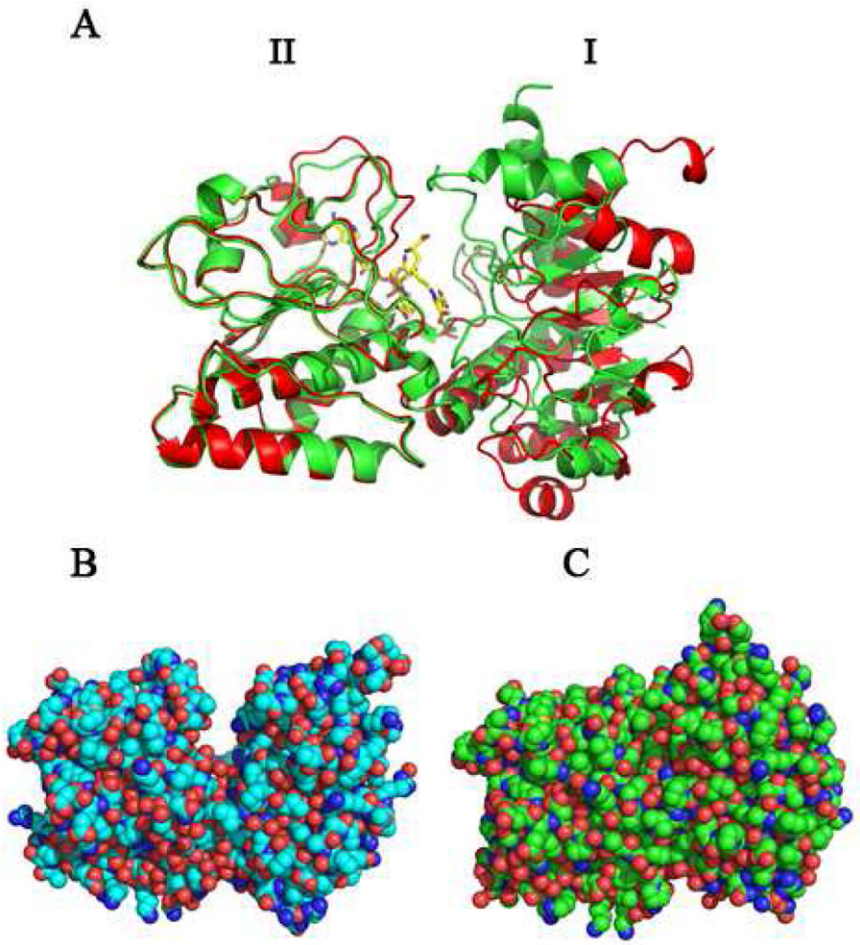

Figure 1.
Overall Structures of the C205S Apo-enzyme and E•NADH•Saccharopine Ternary Complex. A. Superimposition of the apo-enzyme (red) and ternary complex (green) structures. Note the change in the position of the loop and helix in domain I (right) to close the active site. Stick models of NADH and saccharopine are shown bound to domain II (left). B. CPK model of the apo-enzyme with the active site entrance at the top (same orientation as in A). C. CPK model of the ternary complex structure in the same orientation as shown in B.

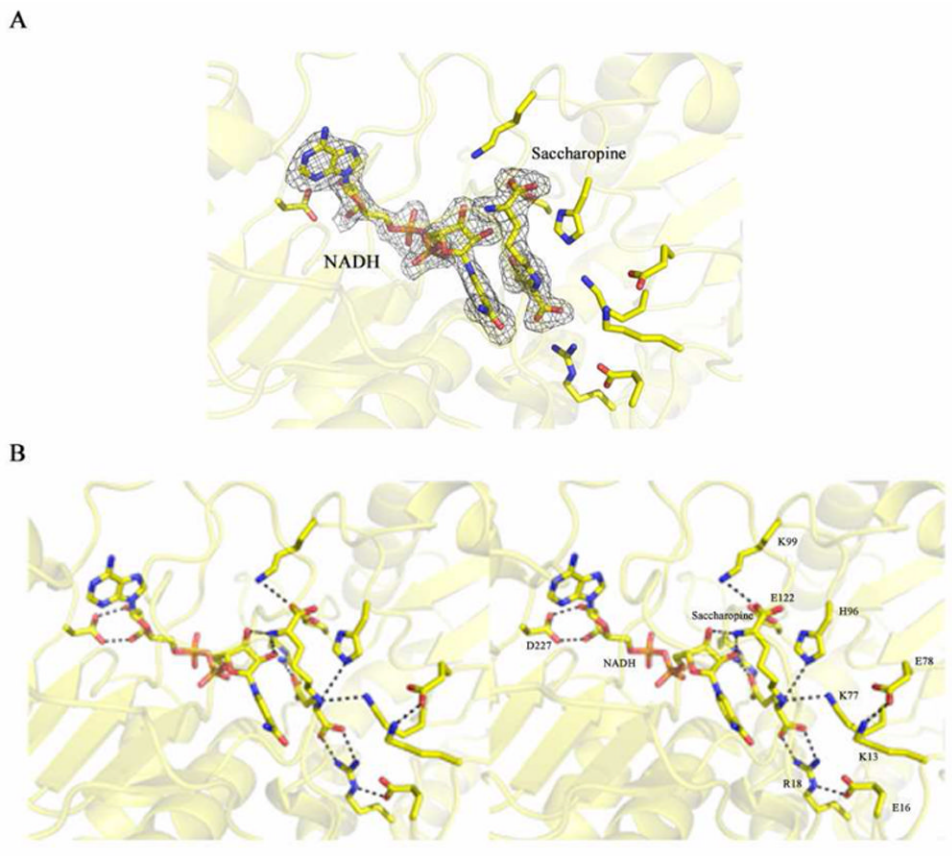

Figure 2.
Close-up view of the Active Site of SDH in the Ternary Complex with NADH and Saccharopine. A. Monoview of a F_o-F_c difference electron density map contoured at 3σ with ligand atoms omitted. B. Stereoview of the active site with NADH and Sacc bound. Residues within hydrogen bond distance (shown as a dashed line) to NADH and Sacc are shown. Distances represented by the dashes are given in Table 4.

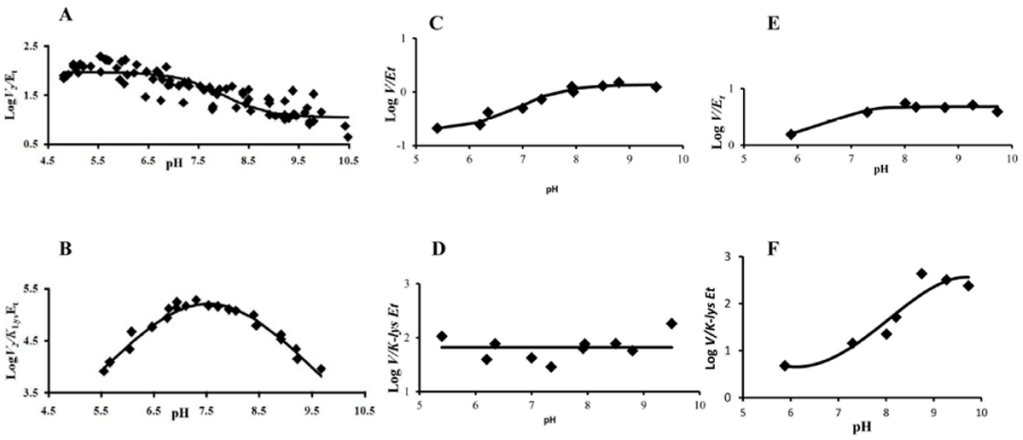

Figure 3.

pH Dependence of Kinetic Parameters for SDH WTSDH (C205S), K77M/C205S and H96Q/C205S in the Direction of Saccharopine Formation. Data for the pseudo WT SDH (C205S)(A and B) are from ref. (1), and are reproduced with permission, while (C and D) are data for the K77M/C205S, (E and F) are for H96Q/C205S mutant enzymes. Units for V/E_t and $V/K\mathbf{E_t}$ are s^{-1} and $M^{-1}\ s^{-1}$, respectively. Points are the experimentally determined values. The curves are theoretical and based on fits to eq. 6 for panel C, E and F.

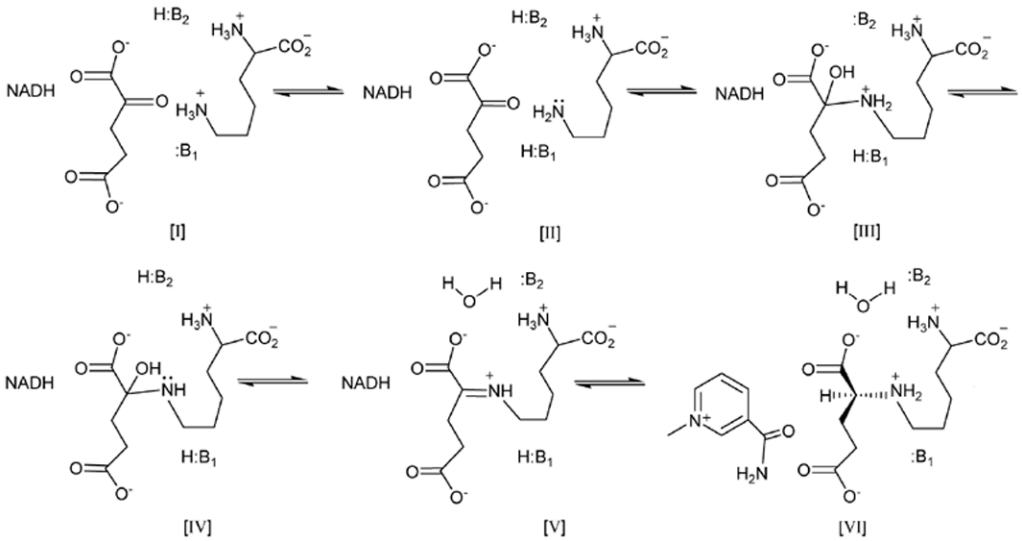

Scheme 1.

Chemical Mechanism Proposed for Saccharopine Dehydrogenase. The reaction is written in the direction of Sacc formation. [I], protonated Lys; [II], the formed central complex E•NADH•α-Kg•Lys; [III], protonated carbinolamine; [IV], carbinolamine intermediate; [V], Schiff base intermediate; [VI], hydride transfer and formation of Sacc. With the exception of Sacc, no stereochemistry is implied.

Table 1

Data Collection Statistics

	C205S apo-enzyme	Sacc/NADH bound
space group	$P2_12_12_1$	$P4_3$
unit cell dimensions (Å)	64.95, 75.23, 75.31	68.88, 68.88, 101.85
wavelength (Å)	1.5418	1.5418
temperature (K)	100	100
resolution (Å)	41.71-2.01(2.12-2.01)	35.2-2.17(2.29-2.17)
no. of observations	98649	89656
no. of unique reflections	24396	25006
completeness (%)	97.1(81.8) [a]	99.8(99.8)
average multiplicity	4.0(2.6)	3.6(3.4)
<I/σI>	15.8(3.0)	14.5(3.4)
R_{merge} [b]	0.052(0.295)	0.063(0.300)
Refinement Statistics		
no. of protein atoms	2921	2884
no. of solvent atoms	152	134
no. of ligand atoms	0	69
avg. B factor (all atoms)	25.01	24.37
R_{cryst} [c]	0.197	0.178
R_{free} [d]	0.273	0.228
rms deviation [e]		
bond length (Å)	0.022	0.022
bond angle (°)	1.74	1.89
Ramachandran plot [f]		
favored	97.8	97.5
allowed	2.2	2.5
outliers	0.00	0.00
disallowed	0.00	0.00

[a] The data in parentheses refer to the highest resolution shell.

[b] $R_{merge} = \Sigma_h\Sigma_i |I_{hi} - \langle I_h \rangle| / \Sigma_h\Sigma_i |\langle I_h \rangle|$. I_{hi} is the *i*th used observation for unique hkl h, and $\langle I_h \rangle$ is the mean intensity for unique hkl h.

[c] $R_{cryst} = \Sigma||F_o| - |F_c|| / \Sigma|F_o|$ where F_o and F_c are the observed and calculated structure factors, respectively.

[d] R_{free} was calculated using 5% of randomly selected diffraction data which were excluded from the refinement.

[e] Ideal values taken from ref. 16

[f] calculated using *MolProbity* (22).

Table 2

Summary of the Kinetic Parameters.

	C205S	K77M[a]	H96Q[a]	K77M/H96Q[a]
$V_2/\mathbf{E_t}$ (s^{-1})	106	0.73 ± 0.02	3.83 ± 0.03	0.16 ± 0.02
$V_2/K_{\alpha\text{-Kg}}\mathbf{E_t}$ ($M^{-1}s^{-1}$	9.7×10^5	73 ± 6	435 ± 116	0.50 ± 0.05
$V_2/K_{Lys}\mathbf{E_t}$ ($M^{-1}s^{-1}$)	1.2×10^5	29 ± 2	14 ± 3	1.7 ± 0.8
$K_{\alpha\text{-}Kg}$ (mM)	0.11	10.0 ± 0.8	9 ± 2	267 ± 60
K_{Lys} (mM)	0.89	25 ± 2	267 ± 60	96 ± 9

[a]Mutations prepared in the C205S background (1).

Table 3

Summary of the Kinetic Isotope Effects[a]

	C205S[b]	K77M[c, d]	H96Q[c, d]
^{D}V	1.3 ± 0.2	1.81 ± 0.02	1.17 ± 0.40
$^{D}(V/K_{Lys})$	1.3 ± 0.2	2.03 ± 0.04	1.17 ± 0.40
^{D2O}V	1.5 ± 0.1	1.45 ± 0.01	2.43 ± 0.02
$^{D2O}(V/K_{Lys})$	1.5 ± 0.1	0.77 ± 0.05	2.43 ± 0.02
$^{D2O}(V)_{D}$	1.5 ± 0.1	1.32 ± 0.02	2.24 ± 0.05
$^{D2O}(V/K_{Lys})_{D}$	1.5 ± 0.1	0.62 ± 0.07	2.24 ± 0.05
$^{D}(V)_{D2O}$	ND	1.42 ± 0.01	1.06 ± 0.11
$^{D}(V/K_{Lys})_{D2O}$	ND	2.03 ± 0.03	1.06 ± 0.11

[a] Isotope Effects were measured at pH 9.

[b] From reference 1.

[c] Errors are standard error of the mean.

[d] Data for K77M were fitted to eq. 4, while data for H96Q were fitted to eq. 3.

Table 4

Distances Between Enzyme Side Chains and Reactants

Side Chain – Reactant	Distance (Å)
R18_NH1 – Sacc_O1	2.8
R18_NH2 – Sacc_O2	2.8
R131_NH1 – Sacc_O3	2.8
R131_NH1 – Sacc_O4	2.6
K77_N^{ε} – Sacc_N^{ε}	3.4
H96_$N^{\varepsilon 2}$ – Sacc_N^{ε}	3.5
K13_ N^{ε} – Q78_O^{γ}	2.6
D227_O1 – NADH_O2	2.6
D227_O1 – NADH_O3	2.8
[a]NADH_4C – Sacc_C8	3.6

[a]Numbering for Sacc is from C1 of the lysine half to C11, the γ-carboxylate of the glutamate half.